



## Supplementary Materials

# Black TiO<sub>2</sub>-Based Dual Photoanodes Boost the Efficiency of Quantum Dot-Sensitized Solar Cells to 11.7%

Danwen Yao <sup>1,†</sup>, Zhenyu Hu <sup>2,†</sup>, Ruifeng Zheng <sup>2</sup>, Jialun Li <sup>2</sup>, Liying Wang <sup>2</sup>, Xijia Yang <sup>2</sup>, Wei Lü <sup>2,\*</sup> and Huailiang Xu <sup>1,3,\*</sup>

<sup>1</sup> State Key Laboratory of Integrated Optoelectronics, College of Electronic Science and Engineering, Jilin University, Changchun 130012, China

<sup>2</sup> State Key Laboratory of Advanced Structural Materials, Ministry of Education, Changchun University of Technology, Changchun 130012, China

<sup>3</sup> State Key Laboratory of Precision Spectroscopy and Chongqing Institute, East China Normal University, Shanghai 200062, China

\* Correspondence: lvwei@ccut.edu.cn (W.L.); huailiang@jlu.edu.cn (H.X.).

† These authors contribute equally to this work.

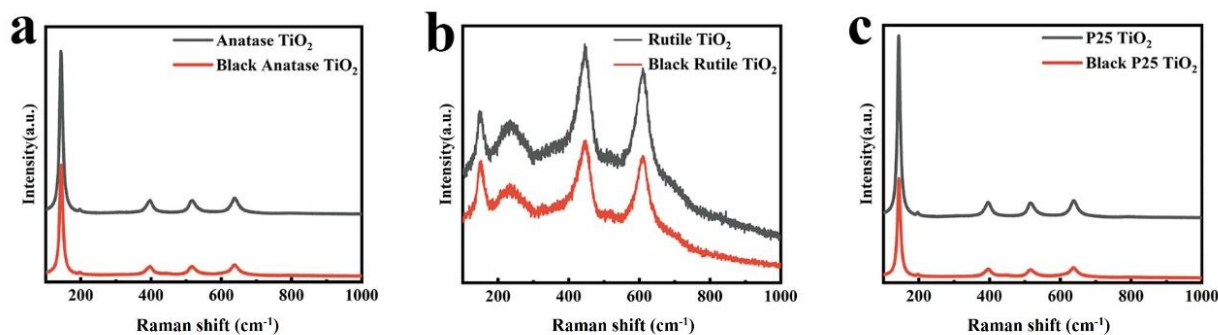


**Figure S1.** (a) Raman spectra of anatase TiO<sub>2</sub> and black anatase TiO<sub>2</sub>. (b) Raman spectra of rutile TiO<sub>2</sub> and black rutile TiO<sub>2</sub>. (c) Raman spectra of P25 TiO<sub>2</sub> and black P25 TiO<sub>2</sub>.

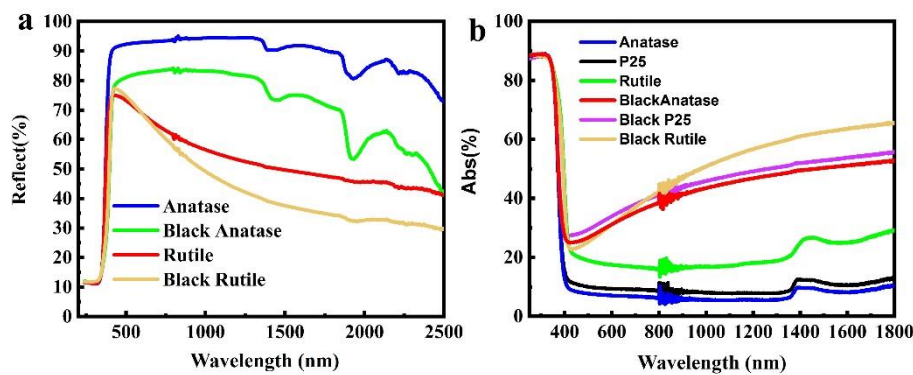


**Figure S2.** (a) Diffuse reflectance spectra of anatase, rutile, P25, black anatase, black rutile, black P25 nanoparticles. (b) Diffuse absorb spectra of anatase, rutile, P25, black anatase, black rutile, black P25 nanoparticles.

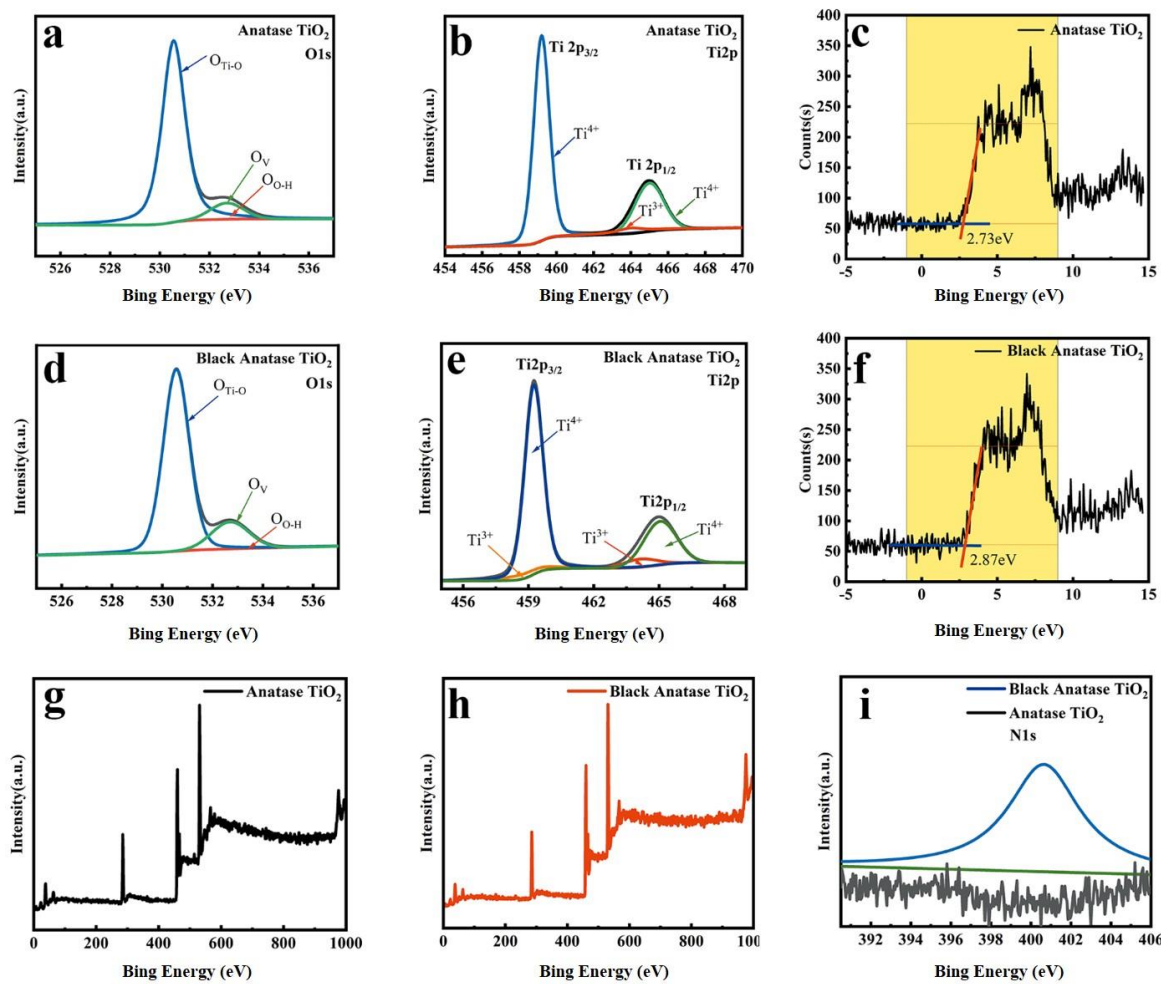


**Figure S3.** (a) O1s XPS spectrum of anatase  $\text{TiO}_2$ . (b) Ti2p XPS spectrum of anatase  $\text{TiO}_2$ . (c) UPS spectrum of anatase  $\text{TiO}_2$ . (d) O1s XPS spectrum of black anatase  $\text{TiO}_2$ . (e) Ti2p XPS spectrum of black anatase  $\text{TiO}_2$ . (f) UPS spectrum of black anatase  $\text{TiO}_2$ . (g) XPS survey of anatase  $\text{TiO}_2$ . (h) XPS survey of black anatase  $\text{TiO}_2$ . (i) N1s XPS spectra of anatase  $\text{TiO}_2$  and black anatase  $\text{TiO}_2$ . The green line is the baseline of the curve.

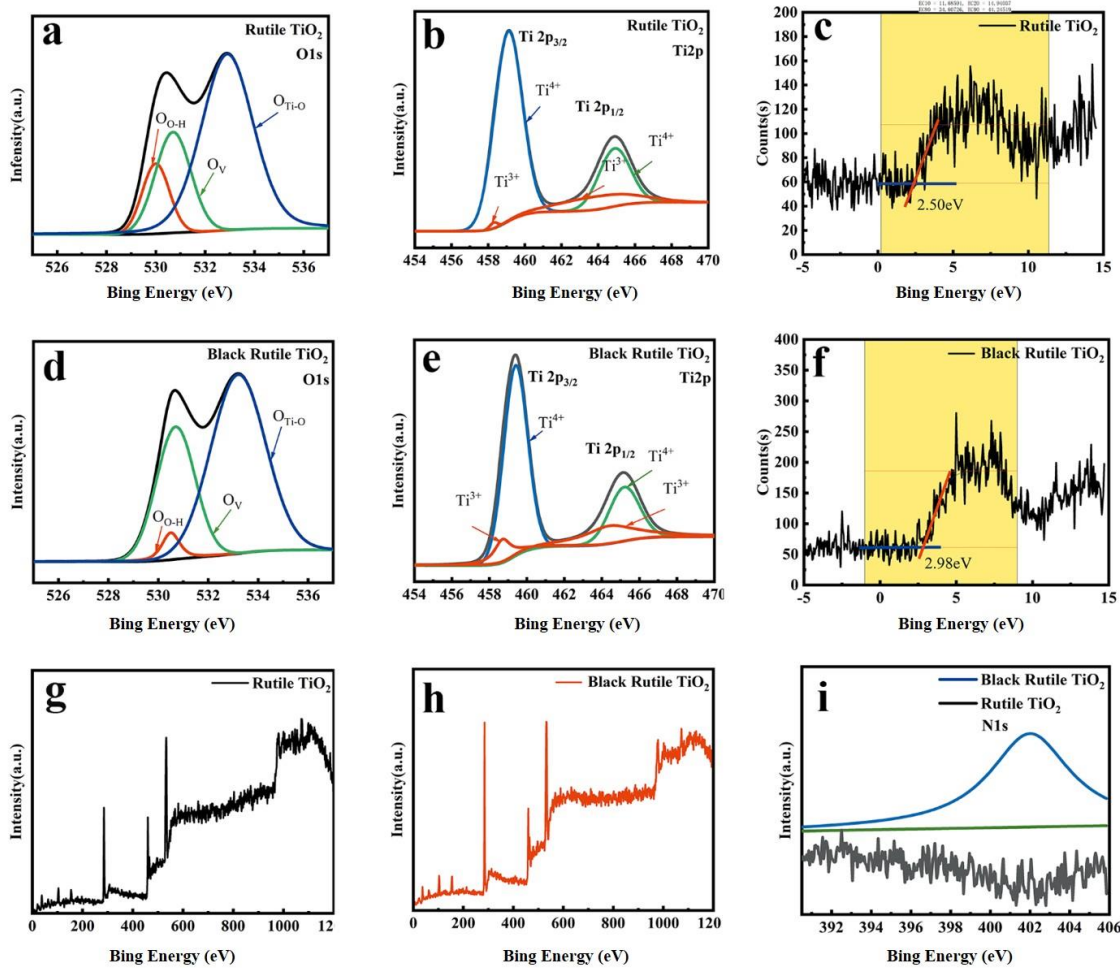


**Figure S4.** (a) O1s XPS spectrum of rutile  $\text{TiO}_2$ . (b) Ti2p XPS spectrum of rutile  $\text{TiO}_2$ . (c) UPS spectrum of rutile  $\text{TiO}_2$ . (d) O1s XPS spectrum of black rutile  $\text{TiO}_2$ . (e) Ti2p XPS spectrum of black rutile  $\text{TiO}_2$ . (f) UPS spectrum of black rutile  $\text{TiO}_2$ . (g) XPS survey of rutile  $\text{TiO}_2$ . (h) XPS survey of black rutile  $\text{TiO}_2$ . (i) N1s XPS spectrum of rutile  $\text{TiO}_2$  and black rutile  $\text{TiO}_2$ . The green line is the baseline of the curve.

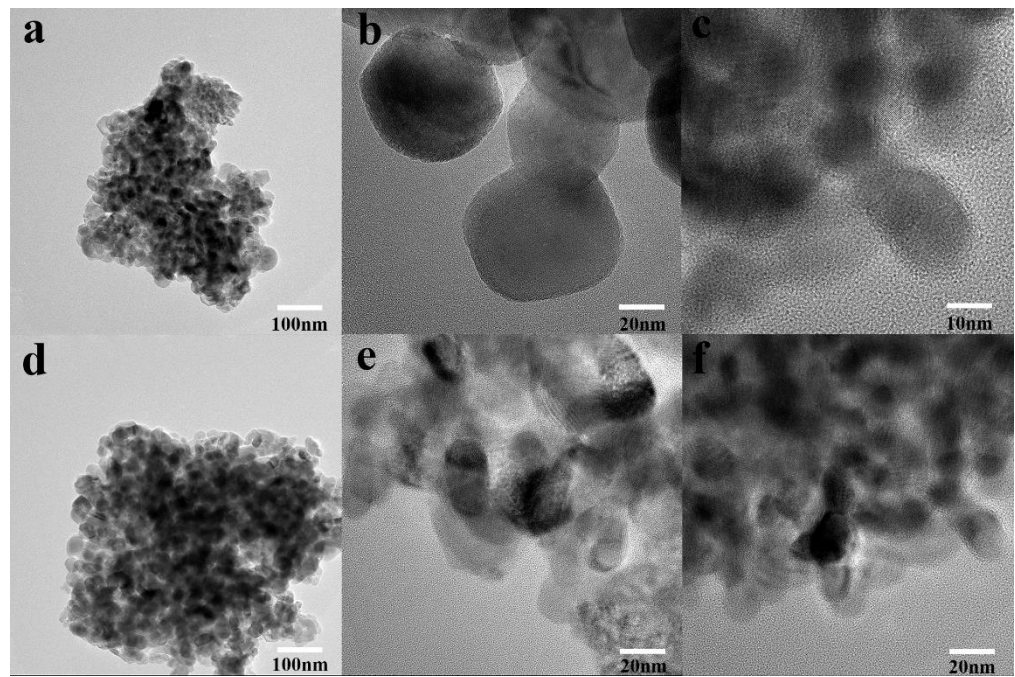


**Figure S5.** TEM and HRTEM images of anatase TiO<sub>2</sub> with different magnifications (a-f).

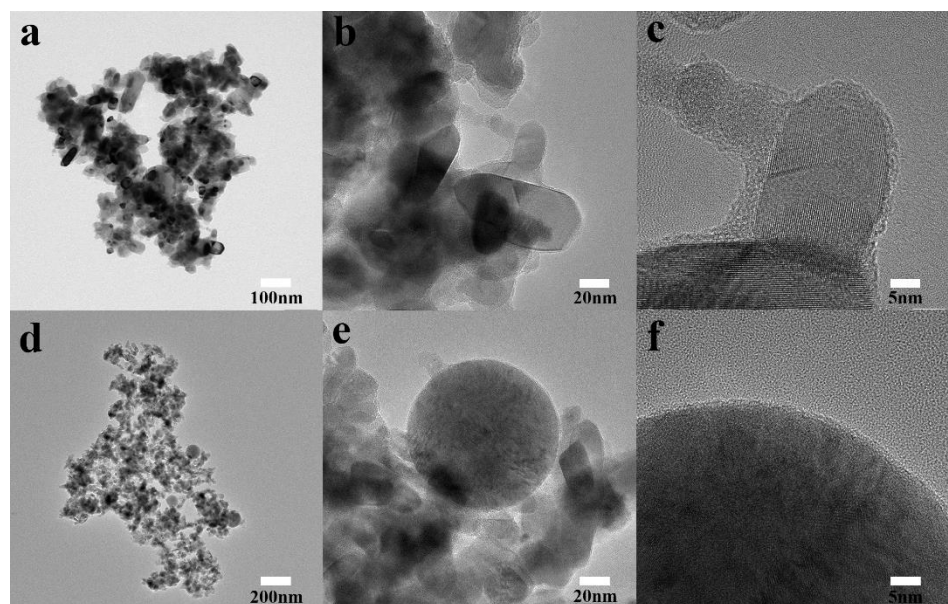


**Figure S6.** TEM and HRTEM images of black anatase TiO<sub>2</sub> with different magnifications (a-f).

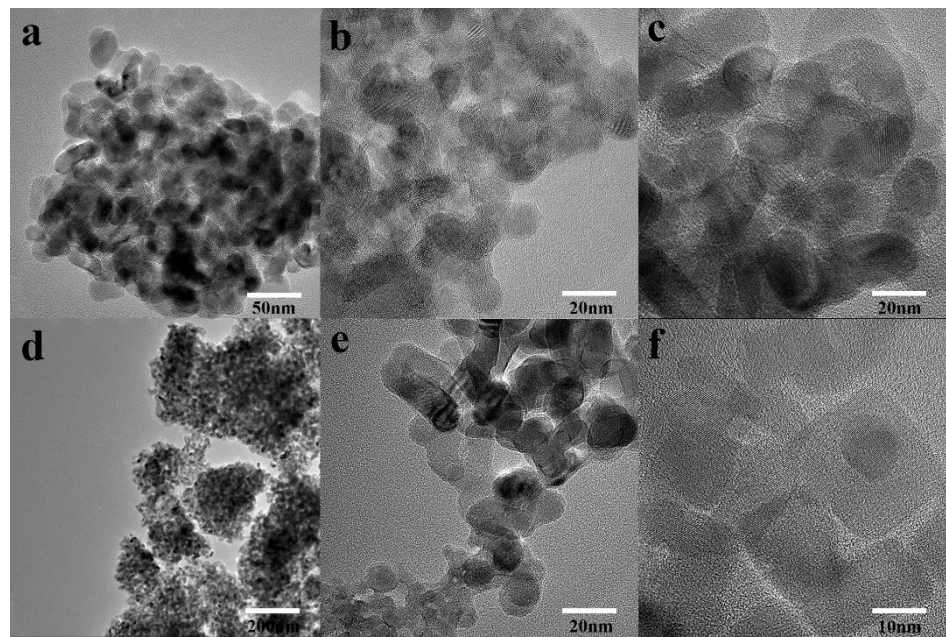


**Figure S7.** TEM and HRTEM images of rutile  $\text{TiO}_2$  with different magnifications (a-f).

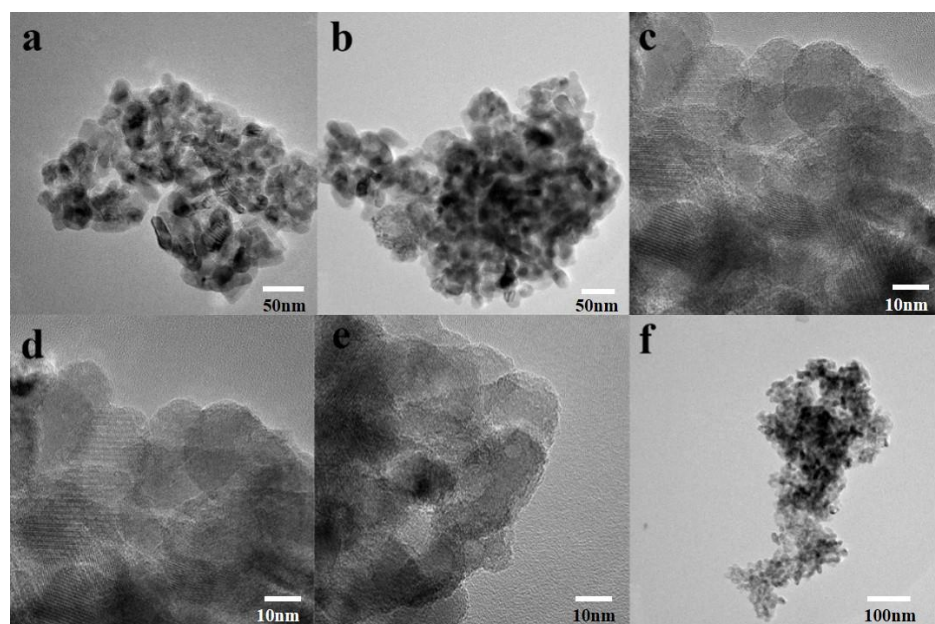


**Figure S8.** TEM and HRTEM images of black rutile  $\text{TiO}_2$  with different magnifications (a-f).

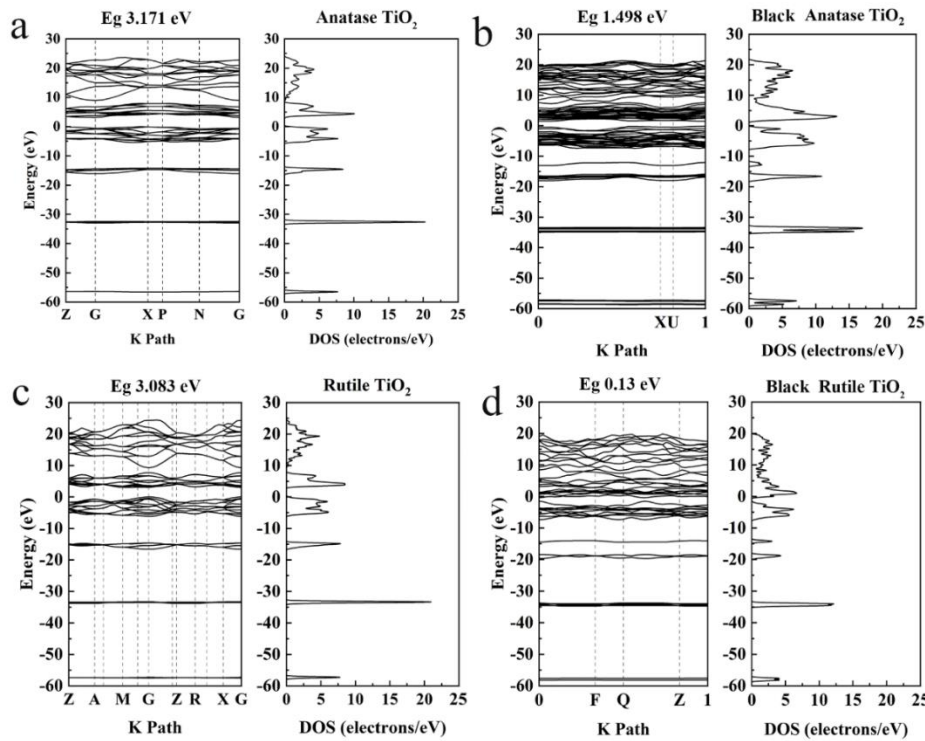


**Figure S9.** Energy band diagram and density of states spectrum obtained by first-principles calculations for (a) anatase  $\text{TiO}_2$ , (b) black anatase  $\text{TiO}_2$ , (c) rutile  $\text{TiO}_2$ , and (d) black rutile  $\text{TiO}_2$ .

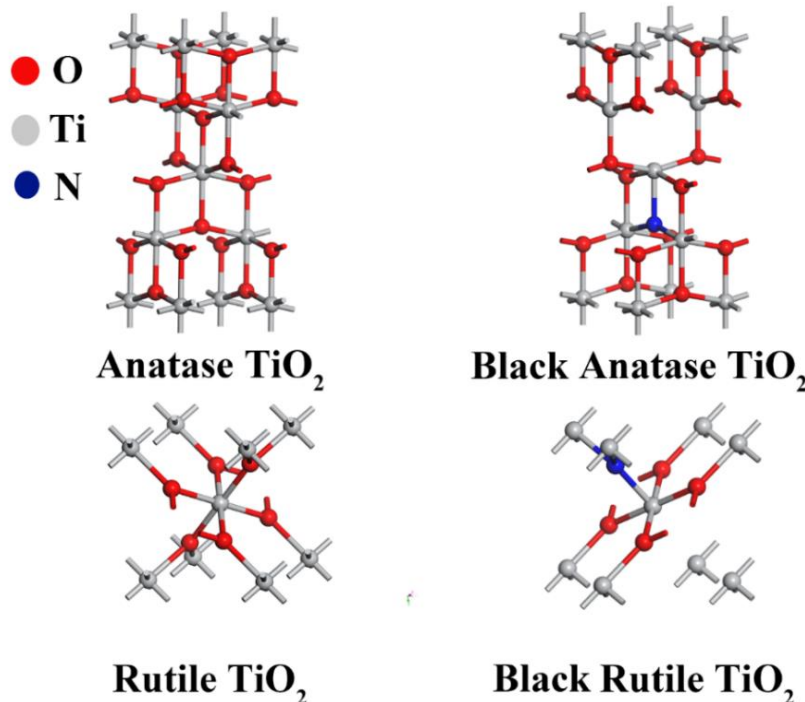


**Figure S10.** Unit cells of anatase  $\text{TiO}_2$ , black anatase  $\text{TiO}_2$ , rutile  $\text{TiO}_2$ , and black rutile  $\text{TiO}_2$  for first-principles calculations.

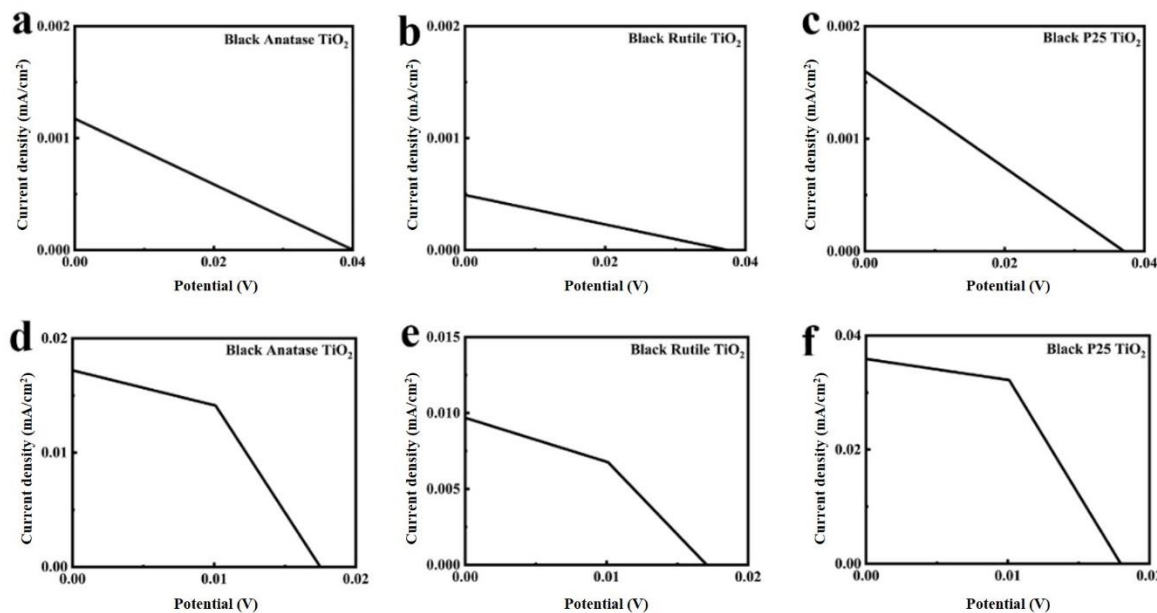


**Figure S11.** (a), (b) and (c) are J-V curves of black anatase  $\text{TiO}_2$ , rutile  $\text{TiO}_2$ , and P25  $\text{TiO}_2$  samples assembled with a  $\text{S}^2/\text{Sn}^{2+}$  electrolyte and copper sulfide counter electrode without quantum dot sensitization. (d), (e) and (f) are J-V curves of black anatase  $\text{TiO}_2$ , rutile  $\text{TiO}_2$ , and P25  $\text{TiO}_2$  samples assembled with a platinum electrode using  $\text{S}^2/\text{Sn}^{2+}$  electrolyte without quantum dot sensitization.

**Table S1.** Performance parameters of CdS/CdSe co-sensitized QDSSCs based on different reports.

Photoanode	QDs	$J_{sc}(\text{mA}/\text{cm}^2)$	$V_{oc}(\text{V})$	FF	PCE(%)	Ref.
TiO <sub>2</sub> NPs	CdS/CdSe	11.91	0.59	0.51	3.56	S1
ZnO NDs/TiO <sub>2</sub> NPs	CdS/CdSe	15.34	0.66	0.53	5.36	S2
TiO <sub>2</sub> NWs-ZnO NSs	CdS/CdSe	16.11	0.51	0.55	4.57	S3
TiO <sub>2</sub> NWs/TiO <sub>2</sub> NSs-ZnO NRs	CdS/CdSe	19.19	0.52	0.54	5.38	S4
TiO <sub>2</sub> MPsNWs	CdS/CdSe	19.32	0.53	0.59	6.01	S5
TiO <sub>2</sub> NWs	CdS/CdSe	17.98	0.47	0.50	4.20	S6
ZnO NDs	CdS/CdSe	16.0	0.62	0.49	4.86	S7
ZnO TP	CdS/CdSe	13.85	0.72	0.42	4.24	S8
ZnO NWs	CdS/CdSe	17.3	0.63	0.38	4.15	S9
TiO <sub>2</sub> /ZnO NSs	CdS/CdSe	16.11	0.51	0.55	4.57	S10
black P25 TiO <sub>2</sub> NDs	CdS/CdSe	25.0	0.61	0.38	5.91	This work
D-G black P25 TiO <sub>2</sub> NDs	CdS/CdSe	50.3	0.61	0.39	11.67	This work

## References

- S1. Kim, S.K.; Raj, C.J.; Kim, H.J. CdS/CdSe quantum dot-sensitized solar cells based on ZnO nanoparticle/nanorod composite electrodes. *Electron. Mater. Lett.* **2014**, *10*, 1137–1142. <https://doi.org/10.1007/s13391-014-4144-0>.
- S2. Jin, B.B.; Wang, Y.F.; Zeng, J.H. Performance enhancement in titania based quantum dot sensitized solar cells through incorporation of disc shaped ZnO nanoparticles into photoanode. *Chem. Phys. Lett.* **2016**, *660*, 76–80. <https://doi.org/10.1016/j.cplett.2016.08.009>.

- S3. Feng, H.L.; Wu, W.Q.; Rao, H.S.; Wan, Q.; Li, L.B.; Kuang, D.B.; Su, C.Y. Three-dimensional TiO<sub>2</sub>/ZnO hybrid array as a heterostructured anode for efficient quantum-dot-sensitized solar cells. *ACS Appl. Mater. Interfaces* **2015**, *7*, 5199–5205. <https://doi.org/10.1021/am507983y>.
- S4. Feng, H.L.; Wu, W.Q.; Rao, H.S.; Li, L.B.; Kuang, D.B.; Su, C.Y. Three-dimensional hyperbranched TiO<sub>2</sub>/ZnO heterostructured arrays for efficient quantum dot-sensitized solar cells. *J. Mater. Chem. A* **2015**, *3*, 14826–14832. <https://doi.org/10.1039/C5TA02269J>.
- S5. Xu, Y.F.; Wu, W.Q.; Rao, H.S.; Chen, H.Y.; Kuang, D.B.; Su, C.Y. CdS/CdSe co-sensitized TiO<sub>2</sub> nanowire-coated hollow Spheres exceeding 6% photovoltaic performance. *Nano Energy* **2015**, *11*, 621–630. <https://doi.org/10.1016/j.nanoen.2014.11.045>.
- S6. Kim, S.K.; Son, M.K.; Park, S.; Jeong, M.S.; Prabakar, K.; Kim, H.J. Surface modification on TiO<sub>2</sub> nanoparticles in CdS/CdSe Quantum Dot-sensitized Solar Cell. *Electrochim. Acta* **2014**, *118*, 118–123. <https://doi.org/10.1016/j.electacta.2013.11.191>.
- S7. Raj, C.J.; Karthick, S.N.; Hemalatha, K.V.; Kim, H.J.; Prabakar, K. Highly efficient ZnO porous nanostructure for CdS/CdSe quantum dot sensitized solar cell. *Thin Solid Films* **2013**, *548*, 636–640. <https://doi.org/10.1016/j.tsf.2013.10.009>.
- S8. Seol, M.; Kim, H.; Tak, Y.; Yong, K. Novel nanowire array based highly efficient quantum dot sensitized solar cell. *Chem Commun (Camb)* **2010**, *46*, 5521–5523. <https://doi.org/10.1039/c0cc00542h>.
- S9. Kim, S.K.; Gopi C.V.V.M.; Rao, S.S.; Punnoose, D.; Kim, H.J. Highly efficient yttrium-doped ZnO nanorods for quantum dot-sensitized solar cells. *Appl. Surf. Sci.* **2016**, *365*, 136–142. <https://doi.org/10.1016/j.apsusc.2016.01.043>.
- S10. Zhao, H.; Huang, F.; Hou, J.; Liu, Z.; Wu, Q.; Cao, H.; Jing, Q.; Peng, S.; Cao, G. Efficiency Enhancement of Quantum Dot Sensitized TiO<sub>2</sub>/ZnO Nanorod Arrays Solar Cells by Plasmonic Ag Nanoparticles. *ACS Appl. Mater. Interfaces* **2016**, *8*, 26675–26682. <https://doi.org/10.1021/acsami.6b06386>.